Journal of Physiology (1990), **422**, *pp.* 561–583
With 9 figures
Printed in Great Britain

THE CALCIUM-DEPENDENT POTASSIUM CONDUCTANCE IN RAT SYMPATHETIC NEURONES

BY O. BELLUZZI AND O. SACCHI

From the Istituto di Fisiologia Generale dell'Università, Via Borsari 46, 44100 Ferrara, Italy

(*Received 18 July 1989*)

SUMMARY

1. Adult and intact sympathetic neurones of isolated rat superior cervical ganglia were subjected to a two-electrode voltage-clamp analysis at 37 °C in order to investigate the Ca^{2+}-dependent K^+ conductance.

2. At each potential a Ca^{2+}-dependent K^+ current, I_{KCa}, was determined as the difference between the current that could be attributed to the voltage-dependent K^+ current, I_{KV}, following Ca^{2+} channel blockade by Cd^{2+} and the total current generated. The final I_{KCa} curves were obtained after correcting the experimental tracings for the underlying I_{Ca} current component.

3. I_{KCa} became detectable during commands to -30 mV. About $3{\cdot}6 \times 10^5$ Ca^{2+} ions are required to enter the cell before I_{KCa} is initiated . The current was modelled on the basis of a 0·4–0·6 ms delay followed by an exponential activation of a fast component, I_{KCaf}, simultaneously with a much slower exponential activation, I_{KCas}. Experiments indicate a sigmoidal activation curve for the fast conductance, g_{KCf}, with half-maximal activation at $-13{\cdot}0$ mV and a slope factor of 4·7 mV (for 5 mM-Ca^{2+} in the bath). The associated time constant, τ_{kcf}, ranged from 0·8 to 2·0 ms. The slow conductance exhibited a similar steady-state activation curve but an activation time constant in the 48–280 ms range. The maximum mean $\bar{g}_{KC}$ was 0·32 μS per neurone for either the fast or slow component.

4. Excess K^+ ions accumulate in the perineuronal space during K^+ current flow giving rise to rapidly occurring, large K^+ reversal potential (E_K) modifications (up to -45 mV for the largest currents). The kinetics of K^+ extracellular load can be described satisfactorily by a simple exponential function ($\tau = 0{\cdot}9$–$2{\cdot}8$ ms). The characteristics of K^+ wash-out appear similar to those of accumulation.

5. The immediate effect of such an extracellular K^+ build-up is to make the apparent I_{KCa} activation kinetics faster and to reduce (up to 50%) the true value of the K^+ conductance. We simulated the predictions of a K^+ diffusion model and generated new functions describing the I_{KCa} steady-state activation, activation rate and maximum conductance values which satisfactorily reconstruct the I_{KCa} current tracings together with the K^+ accumulation process near the membrane.

6. A small component of the Ca^{2+}-dependent K^+ current, I_{AHP}, was observed which survived at membrane potential levels negative to -40 mV. Increasing Ca^{2+} influx by applying longer pulses enhanced I_{AHP}, which on the other hand was also

activated by depolarizations of short duration. This current decayed slowly over hundreds of milliseconds and its amplitude decreased linearly with membrane hyperpolarization with a null point close to E_K.

INTRODUCTION

Calcium-dependent potassium channels have been identified in nearly every excitable cell and voltage-clamp analyses of the Ca^{2+}-related K^+ conductance have been carried out in a variety of neurones, especially invertebrate and vertebrate ganglionic cells (Meech & Standen, 1975; Meech, 1978; Schwarz & Passow, 1983). Relatively less is known about the I_{Ca}–I_{KCa} system in mammalian neurones, although the existence of I_{KCa} is well established (Brown & Griffith, 1983; Freschi, 1983; Galvan & Sedlmeir, 1984; Belluzzi, Sacchi & Wanke, 1985*b*; Hirst, Johnson & van Helden, 1985; Lancaster & Adams, 1986; Segal & Barker, 1986) and single Ca^{2+}-activated K^+ channels have recently been investigated using the patch-clamp technique (Simonneau, Distasi, Tauc & Barbin, 1987; Smart, 1987; Franciolini, 1988). Moreover, at least two types of single-channel K^+ current in excitable membranes have been described which probably are involved in the fast and slow after-hyperpolarizations following one or several action potentials (Blatz & Magleby, 1986; Lang & Ritchie, 1987). Since a kinetic description of the I_{KCa} macrocurrent is still missing, we have now investigated this current in the adult and intact rat sympathetic neurone using the two-electrode voltage-clamp technique. We have previously kinetically characterized the calcium current in voltage-clamped rat sympathetic neurones and reconstructed the precise time course of calcium ion injection during a single action potential (Belluzzi & Sacchi, 1989). We present here an empirical model which potentially describes the behaviour of the related K^+ conductance. Our interest in modelling the I_{KCa} system arises from the observation that there are at least three conductances in this neurone (I_A, I_{KV}, I_{KCa}; transient voltage activated, voltage dependent, calcium dependent) which are alternatively involved in the repolarizing phase of the action potential. The spike falling phase, in fact, is produced by the I_A conductance alone when the spike arises from a hyperpolarized membrane level, whereas the I_{Ca}–I_{KCa} system is mainly responsible for membrane repolarization when the holding potential is reduced and the I_A channels undergo inactivation (Belluzzi, Sacchi & Wanke, 1985*a*). Under these circumstances it is the I_{KCa} that controls the repolarization of the neurone.

In the course of these experiments it was found that the intense K^+ flow during depolarizing pulses resulted in significant modifications of the equilibrium potential for this ion across the membrane. This finding is not new and has been previously described in other systems (Frankenhaeuser & Hodgkin, 1956; Adelman, Palti & Senft, 1973; Adelman & Fitzhugh, 1975; Dubois, 1981; Shrager, Starkus, Lo & Peracchia, 1983; Keynes, Kimura & Greeff, 1988) and also in the present preparation (Belluzzi *et al.* 1985*b*). This effect, however, proved to be so fast during the early flow of outward current that it represented not only a complication in the kinetic description of the potassium conductance in itself, but a systematic component associated with the K^+ movements across the membrane even during a single action potential. The second step of this study, therefore, was to reconsider the kinetic description of I_{KCa} in view of a variable potassium reversal potential, E_K. The data presented here allow a reconstruction of the I_{KCa} time course evoked at different membrane potential levels as well as the prediction of the accompanying E_K modifications.

METHODS

The methods used in this paper are similar to those described in other studies from this laboratory (Belluzzi *et al.* 1985*a*; Belluzzi & Sacchi, 1988). Briefly, superior cervical ganglia were removed under urethane anaesthesia from adult rats and dissected free of connective tissue. The ganglia were then maintained in the recording chamber at 37 °C where they were immersed in continuously oxygenated medium. Individual sympathetic neurones, viewed with Nomarski optics at 500 × magnification, were impaled with two independent microelectrodes and voltage clamped within 2 h after surgery. Microelectrodes filled with 4 M-potassium acetate and with resistances of 25–35 MΩ were used. The perfusion Krebs solution had the following ionic composition (mM): NaCl, 136; KCl, 5·6; $CaCl_2$, 5; $MgCl_2$, 1·2; NaH_2PO_4, 1·2; $NaHCO_3$, 14·3; glucose, 5·5. When the I_{Ca}–I_{KCa} system was analysed, the initial bathing medium was switched to a $H_2PO_4^-$- and HCO_3^--free medium whose composition was (mM): NaCl, 136; KCl, 5·6; $CaCl_2$, 5; $MgCl_2$, 1·2; Tris HCl, 15; glucose, 5·5. Cadmium chloride (0·5 mM) was then included in the perfusing medium without osmotic compensation. All solutions were gassed with 95% O_2 and 5% CO_2 and adjusted to pH 7·3.

A holding potential of −50 mV was used to minimize I_A channel contamination. The current through Na^+ channels was not suppressed; I_{Na} associated with depolarizing voltage steps, on the other hand, always decayed virtually to zero within 1 ms (Belluzzi & Sacchi, 1986). Presentation of pulses and collection of data was via an M24 Olivetti personal computer. Current traces were digitized at 5–10 kHz using a custom-made 15-bit analog-to-digital converter (Analog Devices DAS1153) and stored on disc for analysis. Currents were evoked by a series of pulses in 10 mV steps starting from −30 mV and typically not exceeding +20 mV to avoid significant voltage breakdown. Pulses were separated by 15 s intervals at −50 mV. The major component of delayed outward current in this neurone is sustained by the Ca^{2+}-dependent K^+ conductance. I_{KCa} was thus defined as the fraction of total outward current which is sensitive to the external addition of Ca^{2+} blocking agents and was dissected at each test potential as the difference current obtained by subtracting the current recorded in the presence of 0·5 mM-Cd^{2+} from the current recorded in control solution. The experimental conditions and the media used allowed long-term, stable measurements of Ca^{2+}-mediated conductance mechanisms. Nevertheless some precautions were taken to avoid the effects of deterioration in the quality of recordings. Current responses to individual stimulus episodes were corrected for leakage, measured and scaled from hyperpolarizing pulses applied at the end of each pulse series, prior to current subtraction. (Calcium movements blockade by Cd^{2+} ions had no systematic effect by itself either on the holding current at −50 mV or on the leakage resistance of these neurones.) However, the apparently complete suppression in the difference trace of the Ca^{2+}-independent currents (typically I_{Na}, as illustrated in Fig. 2), evoked at the same membrane potential level before and after exposure to Cd^{2+}, was the main argument to demonstrate that the recording conditions remained stable throughout the experiment.

RESULTS

Membrane depolarization from a holding potential positive to −50 mV evokes two summed outward potassium currents in sympathetic neurones. One of these is due to delayed rectifier channels; the other is dependent on calcium influx and is known as I_{KCa}. In the presence of extracellular Ca^{2+}, I_{KCa} is generally taken as the current component that disappears when the entry of Ca^{2+} through Ca^{2+} channels is precluded; therefore, we added extracellular Cd^{2+}, which is a very effective blocker of Ca^{2+} movements through the membrane in this neurone, and assumed that the remaining K^+ current was equivalent to I_{KV}. Figure 1*A* shows the currents dependent on the presence of external 5 mM-Ca^{2+}. These were obtained at each potential by digitally subtracting the current measured in Cd^{2+} solution from that measured in control solution. The difference traces in Fig. 1*A*, however, represent the complete I_{Ca}–I_{KCa} system and actually comprise two separate current flows: an

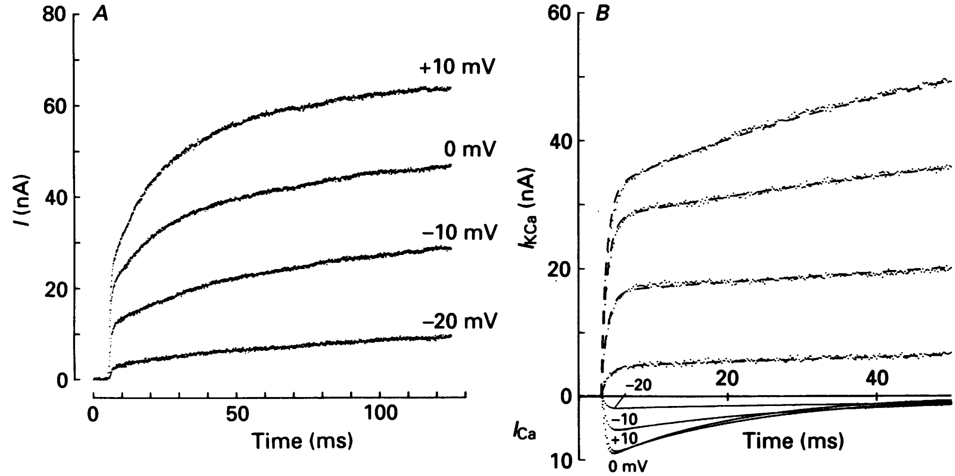

Fig. 1. *A*, dissection of the I_{Ca}–I_{KCa} system in a sympathetic neurone. Superimposed clamp tracings are obtained as difference currents recorded during depolarizing voltage pulses (mV, indicated next to the single traces) before and about 3–5 min after the addition of 0·5 mM-Cd^{2+} to the bath. Holding potential was −50 mV. *B*, relationship between I_{Ca} and I_{KCa} in a sympathetic neurone. Pure I_{KCa} current tracings (upper) are obtained by individually correcting the records shown in *A* for the contaminating I_{Ca} current component reconstructed at the different membrane voltages (lower) according to the I_{Ca} kinetics and neuronal Ca^{2+} permeability described in a preceding paper (Belluzzi & Sacchi, 1989; text eqns (1) and (2) and (4)–(6) with $\bar{P}_{Ca} = 2{\cdot}09 \times 10^{-8}$ cm/s). The dashed lines indicate the best fits of eqn (1) characterizing the summated fast and slow I_{KCa} fractions. Extracellular 5 mM-Ca^{2+} was present throughout.

inward Ca^{2+} current and an outward K^+ current. A small inward Ca^{2+} current preceded I_{KCa} in some traces at lower potentials and at fast speed. Despite the presence of a substantial I_{Ca} in this cell, however, it was not possible to see it directly, as it was largely obscured by I_{KCa}. A reliable detection of any inward currents in this neurone would require very effective blockade of the outward currents. Such experiments were not attempted here in the neurones in which the I_{Ca}–I_{KCa} system was analysed, but by utilizing a previous kinetic characterization of I_{Ca} in this cell (Belluzzi & Sacchi, 1989) it proved relatively simple to reconstruct the individual I_{Ca} evoked by membrane depolarization at different voltage levels and under constant conditions of 5 mM-external Ca^{2+}. The lower traces shown in Fig. 1*B* provide a continuous display of the magnitude of the calcium entry. Subtracting these currents from those of Fig. 1*A* yields the putative pure I_{KCa} tracings, as illustrated in the upper part of the same figure. The generation of uncontaminated I_{KCa} was similarly obtained for five cells. Under these conditions I_{KCa} appeared as a large (> 50 nA) outward current with an activation threshold near −30 mV, which is the membrane potential at which net inward I_{Ca} first became detectable. The initial characterization of I_{KCa} was attempted between -30 and $+20$ mV, the range of potentials relevant to the action potential and the higher voltage at which the current is apparently maximal in our experiments. The I–V curve for I_{KCa} usually has a sigmoidal appearance with a distinct N-shape due to a negative slope conductance. This occurs when calcium influx decreases as the Ca^{2+} equilibrium potential is approached. The definite region of negative slope conductance was not looked for in these experiments. Any inflexion in the steady-state I–V relationship, if present, is however expected to occur at more positive membrane potential levels, much higher than the putative range activated by the physiological action potential amplitude.

The pulse studies presented provide observations on I_{KCa} under conditions of long-lasting calcium influx. The main features of I_{KCa} will be listed here. (1) The time course of the current flow is biphasic: a fast onset is followed by a slower development with maintained membrane depolarization. Outward currents rose steadily during the step, characteristic of the continued activation of I_{KCa}. A comparison of the I_{KCa} and I_{Ca} plots, however, makes it apparent that I_{KCa} was still increasing in amplitude when I_{Ca} was inactivating or actually fully inactivated as if a continuous feeding of I_{KCa} by calcium ions was really unnecessary. (2) I_{KCa} macrocurrent displays a strong voltage dependence: this is clearly demonstrated by the current tracings evoked in Fig. 1*B* at 0 and $+10$ mV. Despite the observation that the I_{Ca} curves evoked at these membrane potentials are virtually identical, the I_{KCa} amplitude increase at $+10$ mV is much larger than predicted by the increase in the driving force on K^+ ions. (3) As previously reported (Belluzzi *et al.* 1985*b*), the slow outward currents (and then presumably I_{KCa}) do not exhibit any voltage-dependent inactivation mechanism at membrane potentials negative to -50 mV. A similar conclusion holds true also for the related I_{Ca} current (Belluzzi & Sacchi, 1989). (4) The calcium concentration of the external medium proved to affect the amplitude of I_{Ca}, larger currents being obtained in solutions with higher calcium concentrations. This is correlated with the calcium dependence of the I_{Ca}. Thus, while changes in the external Ca^{2+} concentration from 2 to 5 mM changed the amplitude of I_{Ca} by a factor of approximately 1·6, the related I_{KCa} measured following standard activation pulses remained virtually unaffected (three cells, not shown). This observation would indicate that the capacity to activate I_{KCa} by the Ca^{2+} entering the neurone during depolarization is rapidly saturated and further Ca^{2+} inflow becomes irrelevant in generating additional K^+ current. (5) I_{KCa} onset occurs with a clear delay. This is illustrated in Fig. 2, in which the I_{Ca}–I_{KCa} system was isolated by the difference current procedure in the same neurone during a 1 or 2 ms voltage step to 0 mV. It is evident from this figure that in this cell I_{KCa} was not measurably activated by pulses shorter than 1 ms, as suggested by the absence of outward tail current components on repolarization to the holding potential either in the individual tracings before and after Cd^{2+} bath immission or in the difference current traces. An inward relaxation is actually detectable. The outward tail current becomes evident only after a 2 ms step duration at 0 mV. There was some variation in this observation in other cells. In six neurones where pulses up to $+20$ mV were applied, pulse widths in the range 0·4–0·7 ms were required to provide measurable I_{KCa}. The delay durations have been compared to the maximum current amplitudes and different pulse voltages but neither factors proved to affect this time shift significantly. These results demonstrate the calcium dependence of I_{KCa}, but they also suggest that relatively little Ca^{2+} entry may be required to cause a maximal activation of the K^+ current, as suggested by the very rapid rise of I_{KCa}. The necessity for an initial delay of about 0·6 ms interposed between the onset of depolarization and that of the

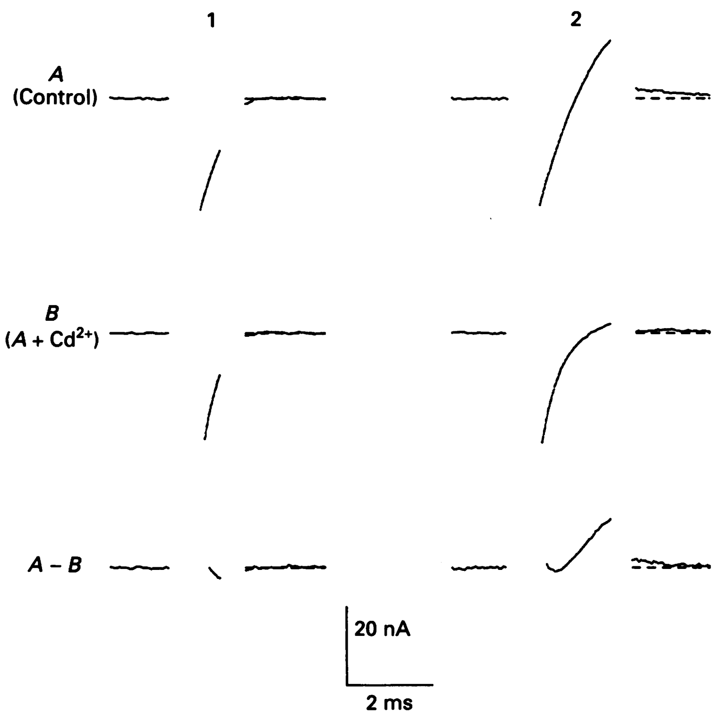

Fig. 2. Time is required to activate I_{KCa}. Membrane currents recorded in a rat sympathetic neurone during voltage-clamp pulses to 0 mV of 1 ms (1) and 2 ms (2) duration from a holding potential of −50 mV. The neurone was bathed in normal saline (row *A*) and in a solution containing 0·5 mM-Cd^{2+} (row *B*). Row *A* − *B* illustrates the corresponding difference tracings. Dashed lines indicate zero current level.

conductance change was confirmed in the least-squares fits to the I_{KCa} tracings as illustrated in Fig. 1*B* (see below). It will be noted that such a delay is at least one order of magnitude larger than that detected in the onset of other currents (I_A, I_{Na}, I_{Ca}) analysed in similar experiments under the same voltage-clamp conditions and which could be simply accounted for by technical factors (response time of the voltage-clamp circuitry, filtering procedures prior to analog-to-digital conversion, presence of capacity transients, etc.). It is most likely that the initial dead phase is physiologically relevant since it actually represents the time required for intracellular Ca^{2+} to activate the K^+ conductance. The percentage of I_{Ca} utilized for priming, assuming a 0·6 ms mean delay, was 30% of the peak calcium current amplitude and corresponds to the entry of some $3{\cdot}6 \times 10^5$ Ca^{2+} ions into the cell. The various experiments with step depolarizations show that the Ca^{2+}-related K^+ conductance is activated to a large extent by very brief periods of Ca^{2+} inflow and that a relatively constant Ca^{2+} load of the neurone may generate greatly increasing I_{KCa} with command pulses of increasing amplitude. If this conclusion is correct, then the voltage dependence of the K^+ conductance must arise primarily from a voltage-dependent activation of K^+ channels by intracellular Ca^{2+}.

We have chosen to fit I_{KCa} with a simple model, in the framework of the Hodgkin–Huxley kinetic scheme (Hodgkin & Huxley, 1952), where the current is considered to rise following a double-exponential function after an initial delay period, δt, of 0·6 ms. Figure 1*B* shows I_{KCa} records and fits obtained by least-squares regression of the function:

$$I_{KCa} = \bar{g}_{KCf}(V-E_K)[1-\exp\{-(t-\delta t)/\tau_{kcf}\}]+\bar{g}_{KCs}(V-E_K)[1-\exp\{-(t-\delta t)/\tau_{kcs}\}], \tag{1}$$

where τ_{kcf} and τ_{kcs} are the fast and slow time constants of the conductance change, $\bar{g}_{KCf}$ and $\bar{g}_{KCs}$ are the corresponding steady-state maximum values of the Ca^{2+}-related K^+ conductances and E_K is the K^+ equilibrium potential which is assumed to be constant at -93 mV. The curves calculated using eqn (1) satisfactorily fit the recordings shown in Fig. 1*B*, provided a time lag is introduced. Figure 3 gives the mean values of the activation parameters in five different experiments. Steady-state g_{KCf} conductances were computed from I_f' values (i.e. current amplitudes of the fast component extracted by the fitting procedure illustrated in Fig. 1*B*) measured at various potentials and normalized to the largest conductance, $\bar{g}_{KCf}$, for each cell. The mean value for $\bar{g}_{KCf}$ from five neurones was $0{\cdot}32 \pm 0{\cdot}05$ μS. Similarly, the $\bar{g}_{KCs}$ values were calculated in the same neurone pool; this conductance attained a mean maximum value of $0{\cdot}31 \pm 0{\cdot}06$ μS per neurone at $+20$ mV. The continuous lines of Fig. 3*A* and *C* are each a plot of the steady-state kc variables as a function of membrane potential, computed according to the equations:

$$\mathrm{kcf}_\infty = 1/\{1+\exp[(-13{\cdot}05-V)/4{\cdot}72]\}, \tag{2}$$

$$\mathrm{kcs}_\infty = 1/\{1+\exp[(-14{\cdot}77-V)/5{\cdot}77]\}. \tag{3}$$

The time constants for the I_{KCa} onset derived by fitting eqn (1) to the tracings were taken as the activation time constants, τ_{kcf} and τ_{kcs}, of the fast and slow conductance components described by eqns (2) and (3). The values are illustrated in Fig. 3*B* and *D* as a function of membrane potential over the voltage range from -20 to $+20$ mV. Values of τ_{kcf} for $V \leqslant -40$ mV were computed by a least-squares curve fit of a single-exponential function to pure I_{KCa} tail relaxations in difference current tracings recorded upon repolarization back to different holding potentials. The depolarizing pulses were maintained short (3 ms) so that only the fast-conductance component of I_{KCa} was presumably activated; the corresponding tail currents, therefore, properly represent the fast activation kinetics. The mean of the values given in Fig. 3 shows that between pulse potentials of -50 and $+20$ mV, τ_{kcf} fell from 1·8 to 0·8 ms, and τ_{kcs} from 280 to 50 ms. As may be seen, the relationships between the activation time constants and voltage are continuous, nearly symmetrical curves, whose maxima occur at about -30 mV (fast activation time constant) and -10 mV (slow time constant). The pooled data over the voltage range examined are fitted by the equations (τ in milliseconds):

$$\tau_{kcf} = 1/[22{\cdot}52\exp(0{\cdot}1060\,V)+0{\cdot}0008665\exp(-0{\cdot}1651\,V)]+0{\cdot}8, \tag{4}$$

$$\tau_{kcs} = 1/[0{\cdot}0855\exp(0{\cdot}6529\,V)+0{\cdot}001618\exp(-0{\cdot}1157\,V)]+75-1{\cdot}5\,V. \tag{5}$$

Equations (1)–(5) provide a description of the Ca^{2+}-dependent K^+ conductance in the rat sympathetic neurone as a function of potential and time. Combining these data with the $\bar{g}_{KC}$ values previously reported a satisfactory reconstruction of the $\bar{I}_{KCa}$ currents evoked at different potentials in voltage-clamp experiments is obtained.

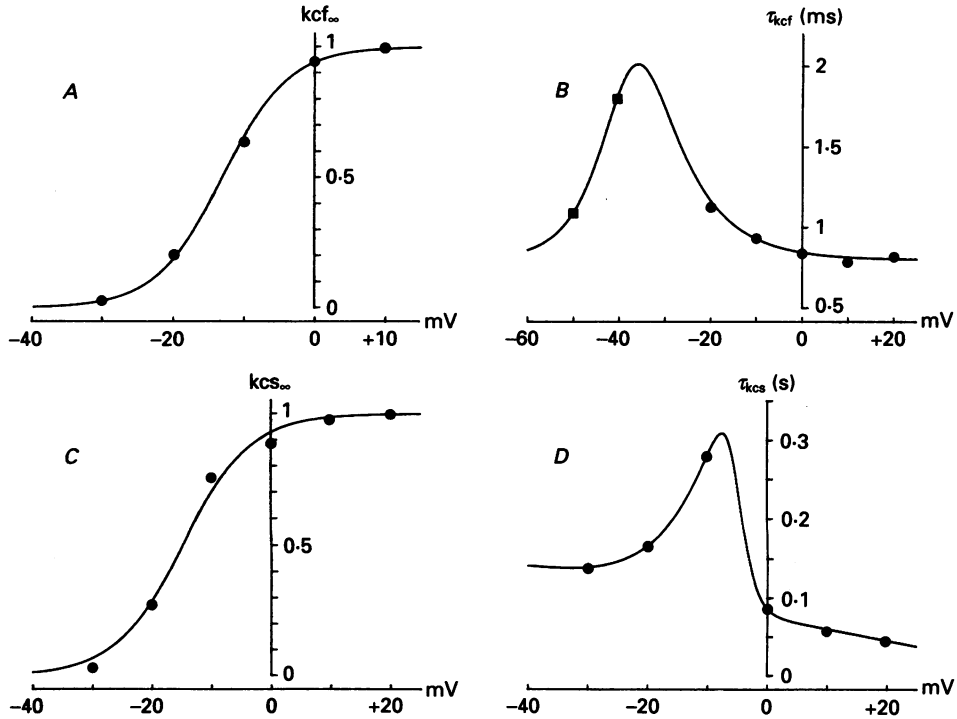

Fig. 3. Kinetic characterization of the I_{KCa} activation mechanism in the rat sympathetic neurone at 37 °C exposed to 5 mM-Ca^{2+} external solution. *A* and *C*, voltage dependence of the fast, kcf, and slow, kcs, steady-state variables from a five neurone sample. The experimental points indicate the normalized mean values of the relative current amplitudes associated with the fast and slow current fractions extracted from tracings like those illustrated in Fig. 1*B*. The continuous curves are the best least-squares fits of eqn (2) and eqn (3) to the fast and slow steady-state activation parameters, respectively. *B* and *D*, τ_{kcf} and τ_{kcs} voltage dependence in sympathetic neurones. Data points represent mean values of the fast and slow current onset time constants obtained from traces similar to those shown in Fig. 1*B* for $V \geqslant -30$ mV (●, $n = 5$). In *B* τ_{kcf} estimates for $V \leqslant -40$ mV are derived from the tail current time course of the difference tracings before and after Cd^{2+} application measured during repolarization at the indicated membrane levels following a 4 ms command pulse to 0 mV (■, $n = 4$). The continuous curves are drawn according to eqn (4) in *B* and eqn (5) in *D*.

External K^+ accumulation and effects on g_{KC}

The previous analysis provides a precise phenomenological description of the I_{KCa} current flow, but is inaccurate in interpreting the intimate events underlying the changes in permeability. In the calculation of g_{KC} as a function of time, in fact, we have assumed that the external K^+ concentration does not vary significantly with current flow. A major source of inaccuracy in these measurements actually arises from the tendency, during the current outflow, for an accumulation of K^+ ions to take place in the extracellular cleft between the neuronal membrane and the inner surface of glial cells. This results in a continuous variation with time of the K^+ equilibrium potential, E_K, which contributes to the driving force for I_{KCa}. Such an effect was first described by Frankenhaeuser & Hodgkin (1956) for the squid giant axon and has since been further investigated in the Ranvier node of the frog (Dubois, 1981), in the crayfish giant axon (Shrager *et al.* 1983), in the CNS of both vertebrates and invertebrates (Kuffler & Potter, 1964; Orkand, Nicholls & Kuffler, 1966; Baylor & Nicholls, 1969) and in frog and rat sympathetic ganglia (Belluzzi *et al.* 1985*b*; Lancaster & Pennefather, 1987).

Figure 4*A* shows a family of tail currents generated in a rat sympathetic neurone on repolarizing to the holding level of -50 mV following a series of 35 ms depolarizing steps in the -10 to $+30$ mV voltage range. The corresponding maximal K^+ current intensities were from 34 to 192 nA. The repolarizing tail tracings revealed increasingly depolarized instantaneous reversal potentials, suggesting large and rapid changes in perineuronal K^+ concentration. The accumulation of K^+ actually resulted in the appearance of an inward tail current for outward currents larger than 80 nA. In Fig. 4*B* and *C* the K^+ reversal potential was measured using a two-pulse voltage-clamp protocol in neurones in which outward currents of two different amplitudes were elicited by a 4 ms step; the membrane was then repeatedly repolarized back to progressively more negative potentials. The instantaneous current–voltage plots for outward current at the end of the command steps were linear over the voltage range tested and exhibited an equilibrium potential value which was the same as the voltage at which reversal of the initial part of the tail tracings occurred. E_K proved to be -78 mV in Fig. 4*B* for the 23 nA peak amplitude current and around -55 mV for the larger current of Fig. 4*C*. By knowing the sizes of the leakage-corrected outward current (I_∞) at the end of various command potentials V_c and the tail current amplitude (I_t) immediately when the voltage was changed from V_c to the repolarized level V_h, the equilibrium potential for K^+ at the end of the pulse was calculated using the equation:

$$E_K = \frac{I_\infty V_h - I_t V_c}{I_\infty - I_t}. \tag{6}$$

This procedure, based on a single voltage-clamp tracing, is sufficiently accurate when compared with the time consuming multistep analysis illustrated in Fig. 4*B* and *C* and so was used in most of these experiments to derive the K^+ reversal potential. We attempted to measure E_K either at the end of a long voltage-clamp pulse in neurones exposed to normal external saline or at the end of short pulses in cells bathed in 0·5 mM-Cd^{2+}. In both cases the tail currents closely reflected the contribution of K^+ movements across the membrane (I_{Ca} is largely or completely inactivated during the long-lasting pulse; I_{Na} is similarly inactivated and I_{Ca} is cancelled by Cd^{2+} treatment in the short duration pulses). The tracings were analysed with the aid of eqn (6) and Fig. 4*D* gives the results of the measurements of this kind made on a number of neurones. As already suggested by previous less extensive observations (Belluzzi *et al.* 1985*b*), it was found that E_K varied continuously with the K^+ outflow and grew

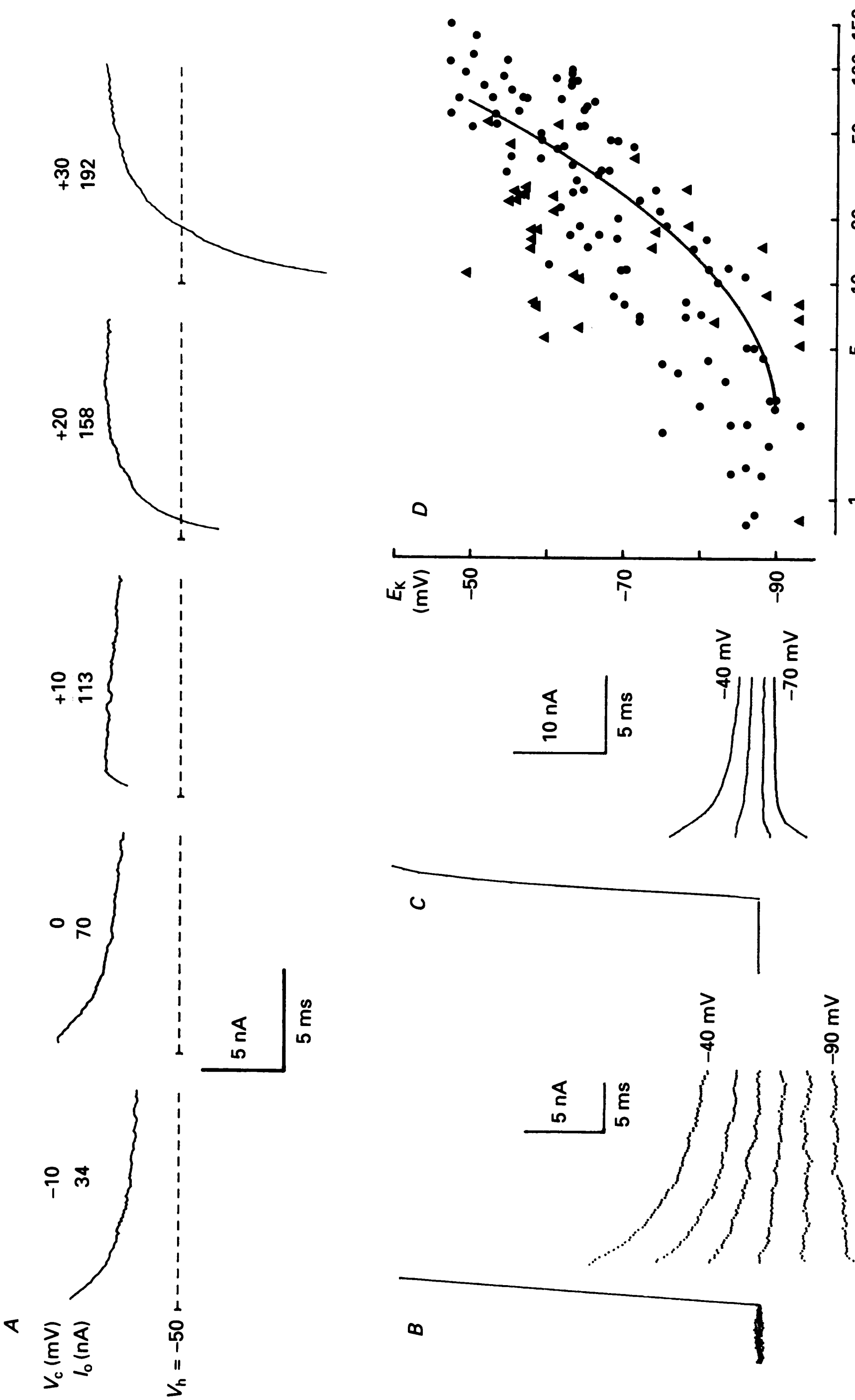

Fig. 4. For legend see facing page.

increasingly positive as the current elicited by the voltage pulse increased. Loading of the perineuronal space by K^+ is measured by the shifts in E_K; the increase in the external K^+ concentration, therefore, can be simply evaluated by the solution of the Nernst equation assuming a constant $[K^+]_i$. This value, however, should be taken with some caution. A 100 nA K^+ current of 300 ms duration, typically obtained upon stepping the membrane to +10 mV, can result in as much as $0{\cdot}31 \times 10^{-12}$ moles of K^+ ions being moved from inside to outside the neurone. This efflux would reduce $[K^+]_i$ by some 35% of the initial value. Therefore, we prefer to indicate the effect of K^+ outflow in terms of modifications of the K^+ concentration gradient across the membrane rather than as a true external K^+ concentration increase; this seems to be correct especially in the case of long-lasting voltage-clamp pulses.

Since the changes in E_K can have the physiological consequence of modifying the currents measured under voltage-clamp conditions, it proved necessary to quantify kinetically the relationship between the K^+ efflux and the extent of E_K modifications. The rate of K^+ loading was estimated from the change in E_K produced during depolarizing pulses of variable duration, after which the tail currents were measured at −50 mV with the usual precaution of extrapolating the exponential part of each tail tracing back to the onset of the repolarizing pulse. Two typical current series are illustrated in Fig. 5. In *A* I_{KV} was elicited at −20 mV and was thus maintained systematically smaller than 4 nA; in *B*, on the contrary, the current evoked was large. In the experiment illustrated in Fig. 5*A* E_K remained close to the resting, theoretical value of −93 mV following a 20 ms pulse and started to shift in a positive direction for longer pulses. E_K changes, however, were limited and resulted in a maximum value of −78 mV when the pulse duration was 160 ms. A different description applies to the large current of Fig. 5*B*; E_K is now drastically and rapidly affected by K^+ outflow. For I_K = 60 nA the calculated value of E_K fell to −65 mV at the end of a 2 ms voltage pulse and appeared to approach a steady-state value

Fig. 4. *A*, tail currents generated on repolarizing to the holding level of −50 mV following a series of 35 ms depolarizing step commands to the voltage levels, V_c, indicated for each tracing. The maximum outward current amplitude, I_0, evoked during the pulse is also reported. The zero-current level is shown for each record. The dashed lines start at the point at which the repolarizing pulse is applied; the 0·5 ms interval in the tracings is obscured by the capacitative current. *B* and *C*, reversal potential of K^+ currents of different intensity in the same 5·6 mM-K^+ external concentration. The cell illustrated in *B* was repeatedly pulsed to 0 mV for 4 ms in the presence of external Cd^{2+} and then repolarized in 10 mV steps in the −40 to −90 mV membrane voltage range. E_K determined either from eqn (6) or from the tail current reversal potential is close to −78 mV. Tracings from a different cell exposed to normal Krebs solution are shown in *C*. The neurone was clamped to +10 mV for 4 ms to evoke larger K^+ currents than in *B*, and tail currents were measured in the −40 to −70 mV post-potential range; E_K is now around −55 mV. Holding potential was −50 mV in both neurones. *D*, K^+ accumulation in the perineuronal space. Semilogarithmic plot of E_K, measured in each record from eqn (6), plotted against the corresponding maximum K^+ current amplitude. Data from twenty-nine different neurones following voltage-clamp pulses in the −30 to +20 mV voltage range of either 390 ms duration in normal Krebs solution (●) or 4–16 ms duration in the presence of 0·5 mM-Cd^{2+} (▲). The continuous curve is the presumed steady-state E_K value calculated from eqn (7) during long-lasting K^+ current flow of different intensities.

within 4 ms. If the command was extended to 16 ms, E_K remained around -57 mV. We plotted in Fig. 5*C* the E_K estimates extracted from the tracings of Fig. 5*B* as a function of the duration of the depolarizing pulse. The K^+ accumulation process proved to be described by a single-exponential function, similar to that detected in

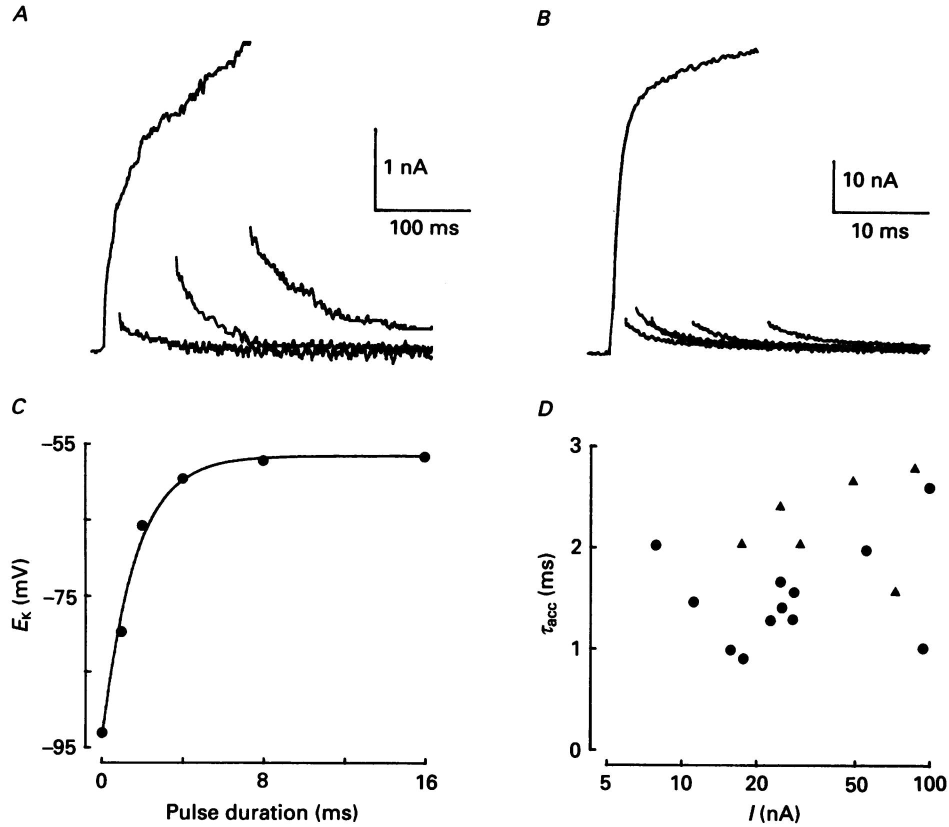

Fig. 5. Effect of K^+ current intensity and duration on E_K. *A*, superposition of three K^+ currents of 20, 80 and 160 ms duration evoked at -20 mV and followed after each pulse by the return to the holding level at -50 mV. E_K was determined for each individual tail current by using eqn (6); the E_K values at the end of the single steps of increasing duration were ~ -93, $-84{\cdot}0$ and $-78{\cdot}6$ mV, respectively. *B*, clamp currents elicited in a different neurone by pulses to 0 mV of 2, 4, 8 or 16 ms duration. *C*, plot of E_K values determined by means of eqn (6) in the experiment partially illustrated in *B* to demonstrate the time course of K^+ loading of the perineuronal space during current flow. E_K is plotted *versus* pulse duration; the time constant of K^+ accumulation, τ_{acc}, is 1·6 ms. *D*, relationship between maximum K^+ current intensity and the time constant of E_K modification, evaluated as in *C*. Data from nine different neurones exposed either to normal saline (●) or after external immission of 0·5 mM-Cd^{2+} (▲).

these and other analyses when the integral of the current was plotted against E_K modifications. In our experiments the time constant of the K^+ load might reflect the time constant of the K^+ current onset; the rate of accumulation, however, proved to be largely independent of current intensity (for currents larger than ~ 5 nA) suggesting that the plot of Fig. 5*C* may represent the kinetics of the balance between

K^+ current flow and K^+ clearance across the glial cell sheath. The K^+ accumulation in the perineuronal space proved to be a very rapid process indeed (Fig. 5*D*); the time constants evaluated in experiments similar to those illustrated in Fig. 5*B* fell within the range 0·9–2·8 ms with a mean value of 1·76 ms (nine neurones, eighteen different

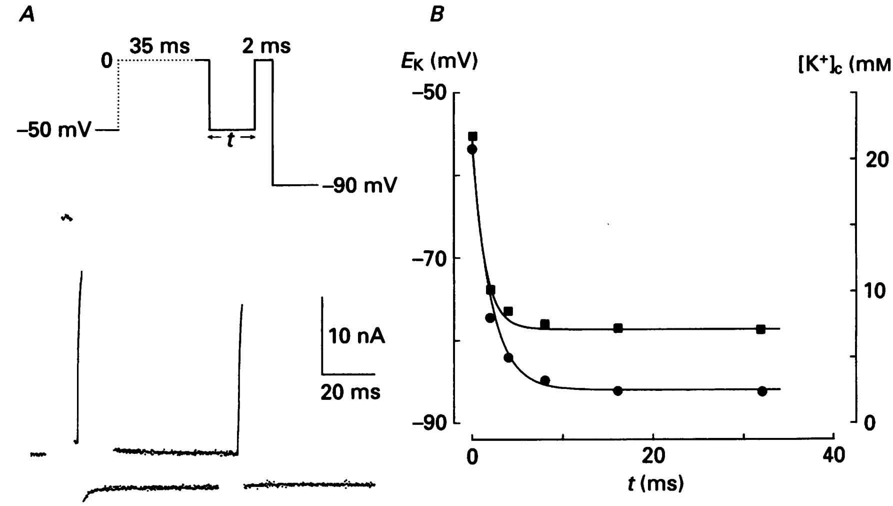

Fig. 6. Rate of wash-out of excess perineuronal K^+ after a voltage-clamp pulse load. *A*, the neurone was repeatedly pulsed to 0 mV for 35 ms to evoke a large K^+ current resulting in significant external K^+ accumulation. E_K was measured at the end of the pulse and at different times after repolarizing to the initial holding level of -50 mV by applying a short test depolarization. The protocol used is shown in the inset. E_K is calculated by means of eqn (6). *B*, time course of K^+ removal from the perineuronal space in the experiment partially illustrated in *A*. E_K values (●) are plotted *versus* the time t during which the neurone was repolarized to -50 mV. The continuous curve shows a single-exponential fit ($\tau = 1{\cdot}9$ ms) to the points. The K^+ reversal potential is converted to concentration of K^+ in the cleft (■; $[K^+]_c$) from the Nernst equation assuming intracellular $K^+ = 182$ mM. Points are similarly fitted by a single-exponential function ($\tau = 1{\cdot}4$ ms).

measurements). In four neurones the E_K value was tested over long-lasting (320 ms) voltage pulses and an additional slow component in E_K shift was detected. The corresponding time constant values were in the 53·7–112·7 ms range and the relative contribution to E_K modification limited to a few millivolts. This slow process, which might be related to a genuine K^+ intracellular depletion (see above), was not further analysed.

Figure 6*A* illustrates an experiment in which the time course of restoration of the perineuronal cleft $[K^+]_c$ level after a conditioning load was analysed. The inset in the figure shows the pulse procedure used to measure the rate of disappearance of excess K^+. A 35 ms depolarizing pulse to 0 mV was given to increase $[K^+]_c$; then the membrane was returned to -50 mV for a variable time (at -50 mV the fast KCa channels will close with a time constant of around 1 ms). A 2 ms test pulse to 0 mV was then applied to reopen a small fraction of K^+ channels with minimal additional injection of K^+ into the perineuronal space. Thereafter the membrane was repolarized to -90 mV. From the test outward current and tail current amplitudes and the leakage repeatedly measured at the different times in which the short test pulses were applied, single E_K values during the K^+ wash-out were calculated by means of eqn (6). A progressively smaller inward tail current was recorded over the first 32 ms following the end of the conditioning pulse, the tail current amplitude becoming almost nil at -90 mV after 64 ms of repolarization at -50 mV. This indicates a virtually complete return of E_K to the initial value. Figure 6*B* shows the results of the experiment partially illustrated in *A*. Both E_K and the calculated Nernstian $[K^+]_c$ values, assuming a minimal K^+ intracellular depletion during the short pre-pulse, are represented. The points are approximated by a single-exponential function; mean data from similar experiments in six different cells yielded a value of 1·94 ms for the time constant describing E_K changes and 1·44 ms when the $[K^+]_c$ parameter is considered. These estimates are in close agreement with the time constant values shown in Fig. 5*D* and indicate that both loading and wash-out of K^+ ions from the perineuronal space are presumably symmetrical processes characterized by very rapid kinetics.

The changes in E_K can be predicted by a multicompartmental model in which K^+ is released from the active neurone into a perineuronal extracellular space of radial width Θ from which K^+ ions diffuse away through a satellite cell barrier of permeability P_K. The increment in K^+ cleft concentration, $[K^+]_c$, compared to that in the bath, $[K^+]_o$, as a function of the K^+ current intensity I_K, was obtained using the following relation (Adelman & Fitzhugh, 1975):

$$\frac{d[K^+]_c}{dt} = (1/\Theta)\,[(I_K/F) - P_K([K^+]_c - [K^+]_o)], \qquad (7)$$

where F is Faraday's constant. We take Θ as 30 nm, in line with similar morphometric and functional estimates of the restricted space thickness that encapsulates neurones and axons. The permeability coefficient of the external barrier was determined either from (Frankenhaeuser & Hodgkin, 1956):

$$P_K = \frac{\tau}{\Theta},$$

where τ is the time constant of rise or decline of $[K^+]_c$, or from the relation (Frankenhaeuser & Hodgkin, 1956):

$$P_K = I_{K\infty}/F([K^+]_{c\infty} - [K^+]_o),$$

where $[K^+]_{c\infty}$ is the cleft K^+ concentration at the end of a long-lasting pulse evoking a K^+ current of final amplitude $I_{K\infty}$ and $[K^+]_o$ is 5·6 mM. Both methods yielded similar results, with slightly smaller values of P_K associated with currents smaller than 20 nA. Therefore, on this basis, we calculate $P_K = 1{\cdot}6 \times 10^{-3}$ cm/s. This result is not too far from the value of $\sim 7 \times 10^{-4}$ cm/s estimated in the squid axon at 4–10 °C (Astion, Coles, Orkand & Abbott, 1988; Keynes *et al.* 1988) if one takes into account the temperature dependence of the diffusion process. Equation (7), together with the indicated values of the constants, reproduces with sufficient accuracy either the final level of E_K displacement during long-lasting K^+ currents of varying intensities (Fig. 4*D*), or the experimental time constant values of accumulation or depletion of K^+ ions in the perineuronal space.

The next question was to estimate the approximate extent of the errors in g_{KC}

kinetic description as illustrated in Fig. 3, which are likely to be related to K^+ external load. A K^+-accumulation-free process has been artificially reproduced by digitally multiplying the experimental points of the tracings recorded during the voltage-clamp pulses by the correction factor $(V-E_{K0})/(V-E_{Kt})$, where E_{K0} is the

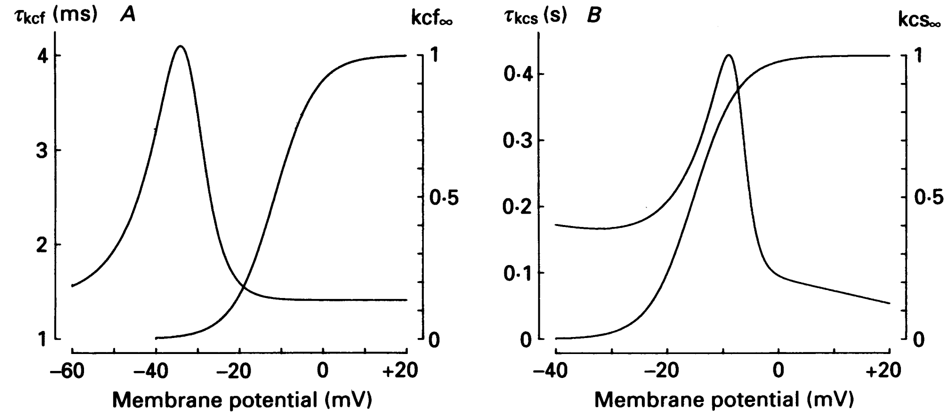

Fig. 7. A and B, steady-state values of the variables kcf and kcs and their time constants τ_{kcf} and τ_{kcs} as a function of membrane potential in the absence of external K^+ accumulation. Continuous lines represent the plot of text eqns (8)–(11); they are derived from the same traces generating the curves of Fig. 3, corrected for K^+ external load according to eqn (7). Numerical values of $\bar{g}_{KCf} = 0{\cdot}45\ \mu S$; of $\bar{g}_{KCs} = 0{\cdot}62\ \mu S$.

resting K^+ equilibrium potential at -93 mV and E_{Kt} is the displaced E_K value after a time t of I_K flow, calculated from the Nernst relation after solving eqn (7) for $[K^+]_c$. This procedure, in principle, reconstructs the I_{KCa} trajectories which would have been recorded in the absence of K^+ accumulation. The same set of I_{KCa} curves giving rise to the kinetic relations shown in Fig. 3 was therefore treated in this manner and least-squares fits were drawn through the corrected data points. New functions presumably describing the true voltage dependence of the activation time constant and the steady-state activation parameters for the fast and slow components of I_{KCa} were thus obtained. The corresponding equations, plotted in Fig. 7A and B, are the following:

$$\mathrm{kcf}_\infty = 1/\{1+\exp[(-11{\cdot}54-V)/4{\cdot}99]\}, \tag{8}$$

$$\mathrm{kcs}_\infty = 1/\{1+\exp[(-15{\cdot}18-V)/4{\cdot}00]\}, \tag{9}$$

$$\tau_{kcf} = 1/[1292{\cdot}4\exp(0{\cdot}274\,V)+0{\cdot}003588\exp(-0{\cdot}1255\,V)]+1{\cdot}41, \tag{10}$$

$$\tau_{kcs} = 1/[0{\cdot}25\exp(0{\cdot}7\,V)+0{\cdot}00073\exp(-0{\cdot}144\,V)]+92-1{\cdot}9045\,V. \tag{11}$$

The mean value for $\bar{g}_{KCf}$ becomes $0{\cdot}45\ \mu S$ and that for $\bar{g}_{KCs}$ $0{\cdot}62\ \mu S$. From these analyses we have no obvious evidence that the K^+ perineuronal load alters the type of I_{KCa} kinetics, but simply that activation develops more slowly (by a factor as large as 2) and, similarly, the maximum conductance values are larger than those obtained using a constant K^+ reversal potential. Therefore, the main apparent result of disregarding the effect of external K^+ accumulation is to make the current activation kinetics appear faster, and to underestimate the conductances. Similar conclusions have been drawn by Adelman *et al.* (1973) and Keynes *et al.* (1988) from experiments in the squid giant axon. An indication of the correctness of this analysis is obtained from the numerical reconstruction of a family of I_{KCa} tracings and their empirical fit to the experimental points of Fig. 1*B*, as illustrated in Fig. 8*A*. E_K was free to

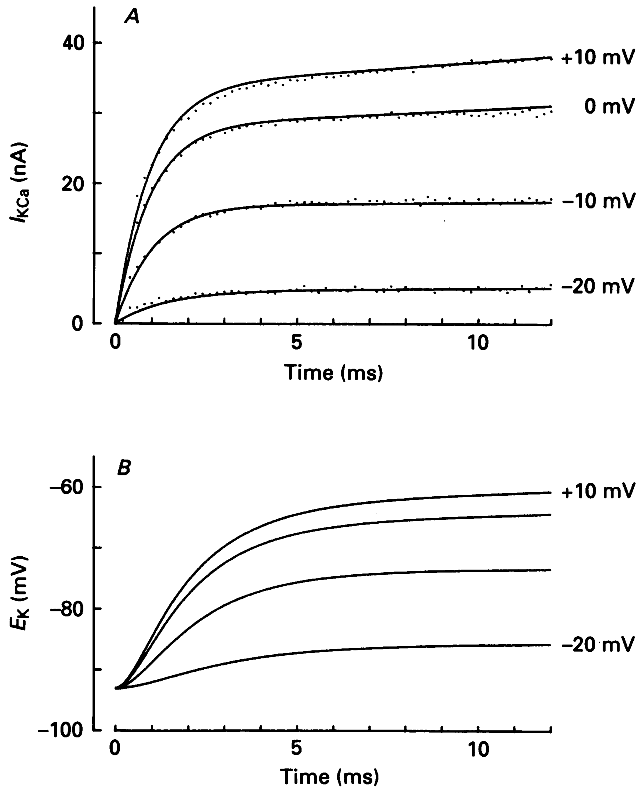

Fig. 8. Computed I_{KCa} tracings together with the accompanying modifications in E_K. *A*, the reconstructed I_{KCa} traces at the indicated membrane potentials are calculated according to text eqns (8)–(11) with $\bar{g}_{KCf} = 0{\cdot}45\ \mu S$ and $\bar{g}_{KCs} = 0{\cdot}62\ \mu S$. Continuous lines are superimposed on the experimental current data points shown in Fig. 1*B* at a slower time base. Holding potential was -50 mV. *B*, time course of E_K shifts during the flow of the corresponding I_{KCa} currents illustrated in *A*. Simulations represent the point-by-point Nernstian E_K values based on the $[K^+]_c$ estimates derived from text eqn (7) and the K^+ intracellular concentration, which was assumed to be constant at 182 mM.

fluctuate, according to eqn (7). In the same figure (*B*) the E_K displacements during the I_{KCa} flow at a variety of membrane potentials are continuously presented. Simulations confirm the fast and large shift in K^+ ions distribution across the neuronal membrane, as revealed in the experiments.

A second Ca^{2+}-activated K^+ current

When the membrane at the end of a voltage-clamp step returns to the holding potential and beyond, the current tracing reveals, in addition to the large short-lived tail currents, a small slow outward component lasting a few hundred milliseconds, as partially illustrated in Figs 4*A* and 5*B*. Experiments indicated that such maintained current was increasingly activated with increasing duration and amplitude in voltage steps. This is illustrated in Fig. 9*A* in a neurone in which the slow tail current was repeatedly measured at -50 mV, 40 ms following the end of depolarizing pulses of varying duration between 5 and 80 ms. The maximum activation in the different

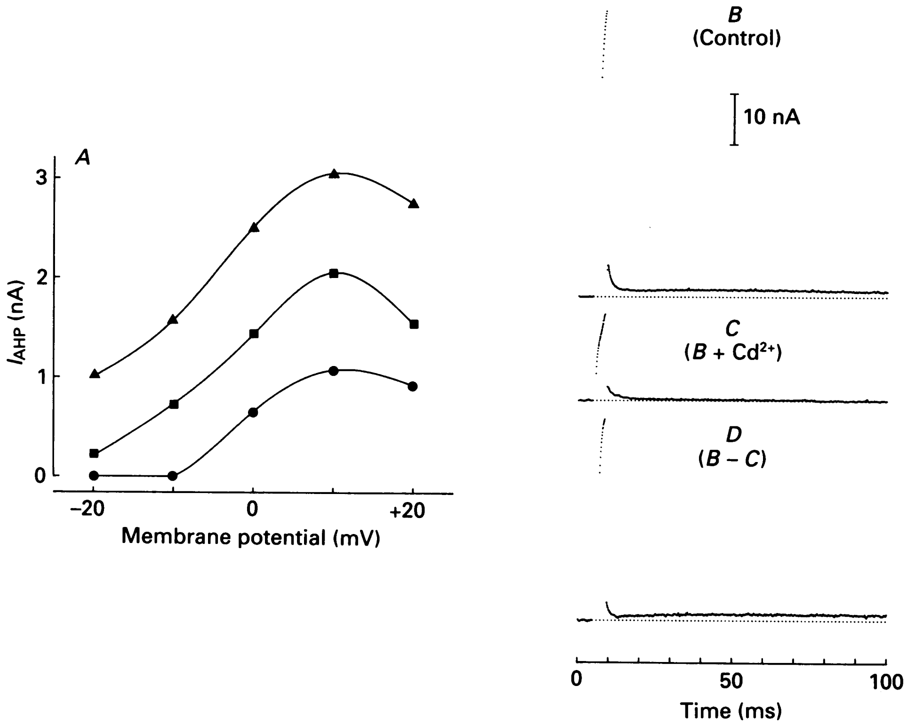

Fig. 9. *A*, I_{AHP} depends on the amount of membrane depolarization and Ca^{2+} load of the neurone. I_{AHP} was measured in the same cell at the holding potential of -50 mV, 40 ms after the end of voltage-clamp pulses of different amplitude and duration (5 (●), 20 (■) or 80 (▲) ms). Normal 5 mM-Ca^{2+} external solution. *B–D*, dissection of the Ca^{2+} – dependent I_{AHP}. The neurone was pulsed for 4 ms to + 10 mV and then returned to the holding potential of -50 mV in the presence of normal 5 mM-Ca^{2+} saline (*B*) and after bath immission of 0·5 mM-Cd^{2+} (*C*). The difference tracing in *D* shows both the fast I_{KCa} and the slow I_{AHP}. Dotted lines indicate zero-current level.

series was observed at $+10$ mV with a peak *I–V* relationship which apparently mirrors that of I_{Ca} (Belluzzi & Sacchi, 1989); by increasing the voltage step length to 80 ms, the maximum amplitude of the slow current at -50 mV was enhanced by a factor of 3 compared to that induced by a 5 ms pulse. The whole current duration, on the other hand, was scarcely affected either by the pulse length or by the membrane potential to which the neurone was brought after the voltage-clamp pulse. Especially in the case of long-lasting depolarization evoking large K^+ currents, the pulse after-effects are the summation of many co-existing processes: (1) the tail current associated with the deactivation of I_{KCaf}; (2) the tail current of I_{KCas}; (3) the restoration of the $[K^+]_c$ and intracellular K^+ concentration; (4) the possible presence of a distinct Ca^{2+}-dependent K^+ current, different from I_{KCa}, and indicated as I_{AHP} from experiments recently performed in bull-frog sympathetic ganglia (Pennefather, Lancaster, Adams & Nicoll, 1985; Tanaka & Kuba, 1987) and in *Aplysia* neurones (Deitmer & Eckert, 1985). I_{KCa} fast channels rapidly turn off at membrane potentials negative to -40 mV. The clearance of K^+ ions from the cleft is similarly a fast process so that these factors appear to be too rapid to account for any of the present observations. We have no direct measurements of the deactivation kinetics of the slow I_{KCa} channels in isolation, but the slow current component could be demonstrated in some cells by applying depolarizing pulses as short as 4 ms, which are expected to minimally activate I_{KCas}. This is illustrated in Fig. 9*B*, in which the slowly decaying component is evoked at $+10$ mV and observed at -50 mV. The pulses are applied in the presence and absence of 0·5 mM-Cd^{2+} so that the difference current clearly indicates the Ca^{2+} dependence of the slow outward current. Similar difference tracings were obtained at various levels of membrane potential; their amplitude decreased linearly with membrane hyperpolarization and were mostly abolished at -90 mV. These results indicate that the slow outward current in this neurone most likely represents a genuine K^+ Ca^{2+}-dependent deactivation current, which differs in voltage sensitivity and activation–deactivation kinetics from those of the conventional I_{KCa}.

DISCUSSION

In this study we employed two-electrode voltage-clamp analysis to characterize some of the properties associated with Ca^{2+}-dependent K^+ conductances expressed in the rat sympathetic neurone. The data presented provide evidence for the existence in this cell of three components of a Ca^{2+}-activated current that can be distinguished by their differing voltage dependence, relative amplitude and activation–deactivation kinetics. The first two components are the fast and slow I_{KCa} fractions activated by depolarization beyond -30 mV and observed in a narrow membrane potential range beyond this level, followed by a third component, I_{AHP}, which survives at negative membrane potentials with an apparent voltage-independent behaviour. The outward K^+ current generated by a depolarizing pulse consists of two phases. Both phases are induced by the activation of a Ca^{2+}-dependent channel which is primed by Ca^{2+} and opened and closed by voltage. We have modelled this current on the basis of a delay followed by an exponential activation of the fast component, concurrent with the much slower exponential activation of a second current component. The model is highly speculative and suffers from the obvious difficulties in obtaining pure I_{KCa} current tracings and the limited understanding of the intimate relationship between Ca^{2+} inflow and I_{KCa} activation. Nevertheless, a particular advantage of the present formulation is that it can be applied in a direct way to define the I_{KCa} participation in the electrical behaviour of the neurone by completing the kinetic description of the five 'major' conductances detected in this neurone and underlying the fast membrane potential shifts during activity (Belluzzi & Sacchi, 1986, 1988, 1989).

With patch-clamp methods at least two distinct and co-existing classes of Ca^{2+}-dependent K^+ channel have been found in excitable membranes (Latorre, Oberhauser, Labarca & Alvarez, 1989) one having a unitary conductance of about 130–300 pS (Marty, 1981) and another having a conductance of about 10–14 pS (cultured rat skeletal muscle, Blatz & Magleby, 1986; GH_3 anterior pituitary cell line, Lang & Ritchie, 1987). Few reports are available on this type of channel in mammalian neurones; the large conductance channels, however, have been described in cultured rat sympathetic neurones (Smart, 1987), cultured rat hippocampal neurones (Franciolini, 1988) and acutely dissociated dorsal root ganglion cells in the neonatal mouse (Simonneau *et al.* 1987). It is tempting to correlate the depolarization-evoked I_{KCa} macrocurrent with the large-conductance BK channels, which apparently share the properties of Ca^{2+} and voltage dependence, non-instantaneous activation and rapid activation–deactivation kinetics. The small conductance SK channels (actually not detected until now in the rat sympathetic neurone) are well suited to sustain the slow I_{AHP} and justify its high Ca^{2+} sensitivity, limited amplitude, slow kinetics, its presence at negative potentials and independence of membrane potential.

The relationship among I_{Ca}, I_{KCa} and I_{AHP} in this neurone may be summarized as follows. I_{Ca} and I_{KCa} share the same voltage dependence and are both dependent on external Ca^{2+}. Although I_{KCa} begins to activate virtually simultaneously with I_{Ca}, it reaches its maximum much later after I_{Ca} has peaked suggesting that I_{KCa} is not critically dependent on electrically detectable I_{Ca}. A possible explanation for this is that the I_{KCa} channel binds Ca^{2+} but such a Ca^{2+}-primed channel is opened and closed by voltage. A priming role of Ca^{2+} was also suggested for a Ca^{2+}-dependent K^+ channel in other cell types. The time required before I_{KCa} becomes measurable provides an estimate of inward Ca^{2+} movements used to activate I_{KCa}. Since the Ca^{2+} which enters the neurone during the voltage-clamp pulse initiates I_{KCa} within 0·6 ms following an injection of about 0·14 pC net inward charge, this sets an upper limit to the internal $[Ca^{2+}]_i$ to initiate the process. This amount of Ca^{2+} would maintain the submembrane $[Ca^{2+}]_i$ sufficiently low to still allow a strong voltage sensitivity of the channel (Barrett, Magleby & Pallotta, 1982; Benham, Bolton, Lang & Takewaki, 1986). We have no direct measure of this sensitivity; the voltage dependence indicated in Fig. 3 might be evaluated, in fact, at $[Ca^{2+}]_i$ which is not rigorously constant. The apparent voltage dependence of 5 mV per e-fold change in conductance is nearly three times as strong as that reported for Ca^{2+}-dependent K^+ channels from cultured hippocampal neurones of rat (Franciolini, 1988). This value would fall at the upper end of the voltage sensitivity range observed in excitable membranes. The whole I_{KCa} current outflow is scarcely dependent on the total amount of Ca^{2+} injected during depolarization, while it is much more influenced by the amount of membrane depolarization. The second phase of Ca^{2+}-dependent K^+ activation, generating I_{AHP}, on the other hand, increases with increasing voltage step duration, and therefore Ca^{2+} load. The limited voltage dependence and slow kinetics suggest that it is similar to the apamin-sensitive Ca^{2+}-activated currents described in other systems and that it might reflect the rate of Ca^{2+} removal or buffering rather than the kinetics of channel closure.

The very different properties of these currents are probably related to the distinctive roles each plays in the electrical behaviour of the neurone. The I_{KCa}, especially its fast component, could be important in restoring the resting membrane potential during an action potential in association with I_A, or in isolation when the I_A channels are inactivated by voltage. From Fig. 3*B* it can be seen that, at potentials near the peak of the spike, I_{KCa} activates with a time constant of about 0·8 ms. On the basis of the conductance value measured, I_{KCa} amplitudes of the order of 30 nA are readily generated within a few milliseconds of membrane depolarization. This amount of current is sufficiently large to account for the repolarizing rate of the cell capacitance (50–80 V/s) observed under current-clamp experiments at holding potentials which inactivate I_A and when repolarization is thus mainly sustained by I_{KCa}. I_{KCa} therefore represents the first major alternative, with regard to speed and intensity, to the I_A repolarization mechanism. It will be reassuring to generate computer simulations of these possibilities; work is in progress in this direction.

We have recently kinetically characterized the I_{Ca} current in the rat sympathetic neurone, reconstructed its participation in spike genesis and evaluated the amount of Ca^{2+} ion entry subsequent to a single action potential. This is about 11·8 pC net inward charge per single spike arising from a -70 mV holding potential, which is largely sufficient to provide the estimated amount of 3×10^5 ions necessary to activate I_{KCa} significantly. No more than a few per cent ($\sim$ 12%) of the total Ca^{2+} movement across the neuronal membrane during a single action potential is thus required to feed the I_{Ca}–I_{KCa} system. The remaining Ca^{2+} would contribute to raise the $[Ca^{2+}]_i$ and presumably activate the long-lasting I_{AHP} which, under current-clamp conditions, generates the prolonged after-hyperpolarization at membrane potentials sufficiently negative to rapidly switch off the I_{KCa}. The pronounced voltage dependence of g_{KC} is of some physiological significance since it means that this conductance can operate under much more favourable conditions to repolarize the membrane from the peak of the action potential than might have been inferred from a rise in $[Ca^{2+}]_i$ following depolarization. These results would suggest that Ca^{2+} and voltage have related effects on I_{KCa} activation, but it is the current's voltage sensitivity that is crucial to its function.

Experiments gave a measure of the mean maximum effective conductance of I_{KCa}. This is about 1·07 μS, as calculated by summating the fast and slow conductance components after correction for K^+ external accumulation. In cell-attached patches on cultured rat sympathetic neurones using equal external and internal K^+ concentration (150 mM) an I_{KCa} single-channel conductance of 200 pS was measured (Smart, 1987). Using a K^+ gradient closer to the physiological ($[K^+]_o = 4·7$ mM), a slope conductance of 120 pS at 0 mV was evaluated. If this latter value is taken as the best estimate of the unitary conductance (the Ca^{2+}-dependent K^+ channel responsible for I_{KCas} was actually not characterized at the single-channel level), then the maximal number of open channels in a sympathetic neurone would be about 8900. This gives a I_{KCa} channel density of four to five channels per square micrometre, which is of the same order as the one to two channels per patch observed from single channel records in cultured neurones.

It is generally accepted that neuronal activity is associated with local changes in extracellular K^+ concentration. A major conclusion of this study, however, is that every process leading to K^+ currents of a few nanoamperes, which represents a small fraction of the total K^+ current power of this neurone, results in fast and significant K^+ external accumulation. The results presented here confirm the early findings of Frankenhaeuser & Hodgkin (1956) with respect to E_K shifts related to the presence of a perineuronal space from which excess K^+ is cleared by a process obeying a simple diffusion equation. The experimental data agree well with such a multi-compartmental model, which accounts for the rate and magnitude of K^+ build-up in this preparation by allowing a quantitative description of the dependence of the extracellular K^+ load on K^+ current flow. The results shown in Figs 7 and 8 indicate that this effect should be considered whenever characterizing a K^+ conductance from membrane currents. The actual conductance values proved in fact to be larger and the conductance turn on–off rates slower than the parameters directly extracted from the rough experimental current tracings. Judging from measurements of changes in E_K, K^+ concentration within the perineuronal space of the sympathetic neurone rose by about 25 mM following a few milliseconds flow of a ~ 80 nA K^+ current. These values of steady-state K^+ load are comparable to data measured in other preparations. For example, in the squid (Keynes *et al.* 1988) K^+ levels increased by 27·4 mM above resting levels at the end of a 30 ms voltage-clamp step to +40 mV. A similar figure (29 mM) was observed in bull-frog sympathetic neurones following a 60 ms pulse to −15 mV (Lancaster & Pennefather, 1987). Less predictable were the practical consequences on E_K of the K^+ current flow associated with normal physiological activity of the neurone. Computed values of the concentration of K^+ ions in the squid periaxonal space indicate that a single action potential increases $[K^+]_o$ by a 1 mM at the peak of the K^+ accumulation process (Adelman & Fitzhugh, 1975). The rat sympathetic neurone spike arising from a holding potential in the −70 to −90 mV voltage range is associated with the injection into the perineuronal space of some 39–55 pC outward charge in less than 2 ms (Belluzzi & Sacchi, 1988). Since Figs 4*D* and 5*D*, and computer simulations quantitatively confirm this result, it follows that the spike-related peak increase in the cleft K^+ concentration will be at least one order of magnitude larger than that expected in the squid giant axon. The mechanisms to minimize external K^+ accumulation (diffusion through extracellular clefts, spatial buffering through coupled glial cells, active K^+ uptake by neuronal and glial membranes) are qualitatively similar in the preparations; equally similar are the dimensions of the perineuronal cleft width and the values of the permeability coefficient of the external diffusion barrier if differences in temperature are taken into account ($3{\cdot}2 \times 10^{-4}$ cm/s at 5 °C for voltage-clamp studies on axons of *Loligo pealei* reported by Adelman *et al.* 1973; $7{\cdot}4 \times 10^{-4}$ cm/s at 4 °C in squid giant axons as estimated by Keynes *et al.* 1988). It would appear that the fast and strong K^+ currents developed by active mammalian neurones have not been accompanied during evolution by parallel improvements in the escape pathways for K^+ ions from the surrounding cleft, so that large and transient external K^+ ion levels actually represent a common feature of normal cell function.

We thank Dr G. Marani for help with the computer. This study was supported by grants from the Ministero della Pubblica Istruzione and Consiglio Nazionale delle Ricerche, Roma.

REFERENCES

ADELMAN, W. J. & FITZHUGH, R. (1975). Solutions of the Hodgkin–Huxley equations modified for potassium accumulation in a periaxonal space. *Federation Proceedings* **34**, 1322–1329.

ADELMAN, W. J., PALTI, Y. & SENFT, J. P. (1973). Potassium ion accumulation in a periaxonal space and its effect on the measurement of membrane potassium ion conductance. *Journal of Membrane Biology* **13**, 387–410.

ASTION, M. L., COLES, J. A., ORKAND, R. K. & ABBOTT, N. J. (1988). K^+ accumulation in the space between giant axon and Schwann cell in the squid *Alloteuthis*. *Biophysical Journal* **53**, 281–285.

BARRETT, J. N., MAGLEBY, K. L. & PALLOTTA, B. S. (1982). Properties of single calcium-activated potassium channels in cultured rat muscle. *Journal of Physiology* **331**, 211–230.

BAYLOR, D. A. & NICHOLLS, J. G. (1969). Changes in extracellular potassium concentration produced by neuronal activity in the central nervous system of the leech. *Journal of Physiology* **203**, 555–569.

BELLUZZI, O. & SACCHI, O. (1986). A quantitative description of the sodium current in the rat sympathetic neurone. *Journal of Physiology* **380**, 275–291.

BELLUZZI, O. & SACCHI, O. (1988). The interactions between potassium and sodium currents in generating action potentials in the rat sympathetic neurone. *Journal of Physiology* **397**, 127–147.

BELLUZZI, O. & SACCHI, O. (1989). Calcium currents in the normal adult rat sympathetic neurone. *Journal of Physiology* **412**, 493–512.

BELLUZZI, O., SACCHI, O. & WANKE, E. (1985*a*). A fast transient outward current in the rat sympathetic neurone studied under voltage-clamp conditions. *Journal of Physiology* **358**, 91–108.

BELLUZZI, O., SACCHI, O. & WANKE, E. (1985*b*). Identification of delayed potassium and calcium currents in the rat sympathetic neurone under voltage clamp. *Journal of Physiology* **358**, 109–129.

BENHAM, C. D., BOLTON, T. B., LANG, R. J. & TAKEWAKI, T. (1986). Calcium-activated potassium channels in single smooth muscle cells of rabbit jejunum and guinea-pig mesenteric artery. *Journal of Physiology* **371**, 45–67.

BLATZ, A. L. & MAGLEBY, K. L. (1986). Single apamin-blocked Ca-activated K^+ channels of small conductance in cultured rat skeletal muscle. *Nature* **323**, 718–720.

BROWN, D. A. & GRIFFITH, W. H. (1983). Calcium-activated outward current in voltage-clamped hippocampal neurones of the guinea-pig. *Journal of Physiology* **337**, 287–301.

DEITMER, J. W. & ECKERT, R. (1985). Two components of Ca-dependent potassium current in identified neurones of *Aplysia californica*. *Pflügers Archiv* **403**, 353–359.

DUBOIS, J. M. (1981). Simultaneous changes in the equilibrium potential and potassium conductance in voltage clamped Ranvier node in the frog. *Journal of Physiology* **318**, 279–295.

FRANCIOLINI, F. (1988). Calcium and voltage dependence of single Ca^{2+}-activated K^+ channels from cultured hippocampal neurons of rat. *Biochimica et biophysica acta* **943**, 419–427.

FRANKENHAEUSER, B. & HODGKIN, A. L. (1956). The after-effects of impulses in the giant nerve fibres of *Loligo*. *Journal of Physiology* **131**, 341–376.

FRESCHI, J. E. (1983). Membrane currents of cultured rat sympathetic neurons under voltage clamp. *Journal of Neurophysiology* **50**, 1460–1478.

GALVAN, M. & SEDLMEIR, C. (1984). Outward currents in voltage-clamped rat sympathetic neurones. *Journal of Physiology* **356**, 115–133.

HIRST, G. D. S., JOHNSON, S. M. & VAN HELDEN, D. F. (1985). The slow calcium-dependent potassium current in a myenteric neurone of the guinea-pig ileum. *Journal of Physiology* **361**, 315–337.

HODGKIN, A. L. & HUXLEY, A. F. (1952). A quantitative description of membrane currents and its application to conduction and excitation in nerve. *Journal of Physiology* **117**, 500–544.

KEYNES, R. D., KIMURA, J. E. & GREEFF, N. G. (1988). Kinetics of activation of the potassium conductance in the squid giant axon. *Proceedings of the Royal Society* B **232**, 375–394.

KUFFLER, S. W. & POTTER, D. D. (1964). Glia in the leech central nervous system: physiological properties and neuron–glia relationship. *Journal of Neurophysiology* **27**, 290–320.

LANCASTER, B. & ADAMS, P. R. (1986). Calcium–dependent current generating the after-hyperpolarization of hippocampal neurons. *Journal of Neurophysiology* **55**, 1268–1282.

LANCASTER, B. & PENNEFATHER, P. (1987). Potassium currents evoked by brief depolarizations in bull-frog sympathetic ganglion cells. *Journal of Physiology* **387**, 519–548.

LANG, D. G. & RITCHIE, A. K. (1987). Large and small conductance calcium-activated potassium channels in the GH_3 anterior pituitary cell line. *Pflügers Archiv* **410**, 614–622.

LATORRE, R., OBERHAUSER, A., LABARCA, P. & ALVAREZ, O. (1989). Varieties of calcium-activated potassium channels. *Annual Review of Physiology* **51**, 385–399.

MARTY, A. (1981). Ca-dependent K channels with large unitary conductance in chromaffin cell membranes. *Nature* **291**, 497–500.

MEECH, R. W. (1978). Calcium-dependent potassium activation in nervous tissues. *Annual Review of Biophysics and Bioengineering* **7**, 1–18.

MEECH, R. W. & STANDEN, N. B. (1975). Potassium activation in *Helix aspersa* neurones under voltage clamp: a component mediated by calcium influx. *Journal of Physiology* **249**, 211–239.

ORKAND, R. K., NICHOLLS, J. G. & KUFFLER, S. W. (1966). Effect of nerve impulses on the membrane potential of glial cells in the central nervous system of amphibia. *Journal of Neurophysiology* **29**, 788–806.

PENNEFATHER, P., LANCASTER, B., ADAMS, P. R. & NICOLL, R. A. (1985). Two distinct Ca-dependent K currents in bullfrog sympathetic ganglion cells. *Proceedings of the National Academy of Sciences of the USA* **82**, 3040–3044.

SCHWARZ, W. & PASSOW, H. (1983). Ca^{2+}-activated K^+ channels in erythrocytes and excitable cells. *Annual Review of Physiology* **45**, 359–374.

SEGAL, M. & BARKER, J. L. (1986). Rat hippocampal neurons in culture: Ca^{2+} and Ca^{2+}-dependent K^+ conductances. *Journal of Neurophysiology* **55**, 751–766.

SHRAGER, P., STARKUS, J. C., LO, M.-V. C. & PERACCHIA, C. (1983). The periaxonal space of crayfish giant axons. *Journal of General Physiology* **82**, 221–244.

SIMONNEAU, M., DISTASI, C., TAUC, L. & BARBIN, G. (1987). Potassium channels in mouse neonate dorsal root ganglion cells: a patch-clamp study. *Brain Research* **412**, 224–232.

SMART, T. G. (1987). Single calcium-activated potassium channels recorded from cultured rat sympathetic neurones. *Journal of Physiology* **389**, 337–360.

TANAKA, K. & KUBA, K. (1987). The Ca^{2+}-sensitive K^+-currents underlying the slow after-hyperpolarization of bullfrog sympathetic neurones. *Pflügers Archiv* **410**, 234–242.